IEEE Access
Multidisciplinary | Rapid Review | Open Access Journal

Received 13 January 2024, accepted 21 January 2024, date of publication 26 January 2024, date of current version 20 February 2024.

Digital Object Identifier 10.1109/ACCESS.2024.3358866

RESEARCH ARTICLE

Speed Regulation of PMSM Systems Based on a New Sliding Mode Reaching Law

HANQING WANG[1], TICAO JIAO[1], XUENING XING[1], AND YANGUANG YANG[2]
[1]School of Electrical and Electronic Engineering, Shandong University of Technology, Zibo 255000, China
[2]Changyi Power Supply Company of State Grid Shandong Electric Power, Weifang 261300, China

Corresponding authors: Ticao Jiao (ticaojiao@gmail.com) and Xuening Xing (xxn@sdut.edu.cn)

This work was supported in part by the National Science Foundation of China under Grant 62073200 and Grant 52377109, and in part by the Taishan Scholar Project of Shandong Province under Grant TSQN202306191 and Grant TSQN202306181.

ABSTRACT This paper is concerned with the speed regulation of permanent magnet synchronous motor systems using sliding mode control. To deal with the contradiction between reaching speed and chattering while ensuring finite time convergence, a new sliding mode reaching law is designed by introducing a variable gain associated with system states. Based on this, a speed regulation controller is first designed for permanent magnet synchronous motor systems using the new reaching law to solve the speed regulation problem and improve system robustness. A rigorously theoretical proof is provided for the designed speed controller using our proposed practical finite time stability criterion. We further investigate the speed estimation of permanent magnet synchronous motors without mechanical sensors. To obtain more accurate rotor information, a new sliding mode observer is designed by incorporating a back electromotive force observer, whose validity is verified by Lyapunov theory. Finally, the correctness of our developed theory is verified through simulation studies.

INDEX TERMS Permanent magnet synchronous motor, new sliding mode reaching law, sliding mode controller, sliding mode observer.

I. INTRODUCTION

Due to the rapid development of science and technology, permanent magnet synchronous motors (PMSMs) have demonstrated remarkable performances, such as simple structure, high power density, and high efficiency. Because of these advantages, it has been extensively employed in various industrial regions, such as electric vehicles, intelligent robots, and industrial automation [1]. At the same time, PMSMs are also a challenging control object with nonlinearity, strong coupling, and multiple variables, making it vulnerable to the effects of unmodeled dynamics, parameter changes, and load disturbances [2], [3].

Proportional integral (PI) as a classical linear control method has been employed to regulate the speed of PMSMs [4]. Due to the dependence on the accuracy of system models, PI control is sensitive to disturbances and parameter changes in the systems. To address these issues, many nonlinear control methods have been proposed and developed, including fuzzy control [5], predictive control [6], neural network control [7] and sliding mode control (SMC) [8], [9], [10]. Compared with the control methods mentioned above, SMC has been widely researched and developed because of its low requirement for system model accuracy and high robustness to internal and external perturbations.

However, the problem of chattering due to high-frequency switching of the system states in the sliding surface region has to be considered in the SMC. To suppress chattering and improve convergence speed, various methods have been proposed, including high-order sliding mode [11] and fractional-order sliding mode [12]. One of the very effective measures to solve it is by improving the sliding mode reaching law [13], [14]. In [8], a new sliding mode reaching law was proposed in which a variable gain was introduced. In [15], a power-reaching law was proposed to achieve chattering reduction and increase convergence rate. In [16], a new

The associate editor coordinating the review of this manuscript and approving it for publication was Zhiguang Feng.

adaptive terminal sliding mode reaching law was introduced and applied to continuous fast terminal sliding mode control. Although chattering reduction, convergence speed improvement, and finite time convergence have been individually achieved in the references mentioned above, they have not been simultaneously considered. Therefore, it is a subject of research interest that they are improved at the same time.

In addition, the acquisition of the rotor position in the PMSM speed regulation systems is important. The rotor information can be obtained by applying an arctangent to the back electromotive force (back EMF), which eliminates the need for mechanical sensors [17]. This method not only eliminates the adverse effects of the environment on mechanical sensors but also reduces the application cost. Therefore, sensorless driving methods have been proposed and developed for middle-speed and high-speed estimations, including extended Kalman filter (EKF) [18], model reference adaptive system (MRAS) [19], [20] and sliding mode observer (SMO) [21], [22]. Although the effectiveness of the EKF in noisy environments is achieved, its calculations are complex, while the MRAS can deliver high accuracy but demands precise models and parameters. Unlike the two methods, the SMO is insensitive to parameter changes and owns strong robustness. Therefore, the SMO has been widely studied and preferred due to its good performance. In [23], a sigmoid function was proposed to suppress chattering, based on which a SMO was designed. In [24], a super-twisting function was designed to replace the signum function to reduce switching amplitude and increase robustness. In [25], a fuzzy adaptive algorithm was proposed to reduce the observation error. In the aforementioned references, although chattering reduction and observation accuracy improvement have been achieved, the design complexity is overlooked. In other words, it makes more sense to simultaneously study the reduction of chattering and observation errors without complicating the design process.

This paper aims to study the speed control performance of permanent magnet synchronous motor speed regulation systems. Firstly, a new sliding mode reaching law (NSMRL) is proposed. Based on this, a new sliding mode controller (NSMC) is designed to ensure that finite time speed regulation is achieved for PMSM systems even in the presence of bounded disturbances. Additionally, a new sliding mode observer (NSMO) is designed to observe the back EMF. Finally, the effectiveness of the designed controller and observer is verified by simulations. The main contributions of this paper are summarized as follows:

1) A new reaching law is designed in which a system state-dependent variable gain is introduced. To demonstrate finite time convergence, a new practical stability criterion is proposed.
2) To address the speed regulation of PMSM systems with perturbations, a NSMC is designed based on our proposed NSMRL and an extended state observer. According to the developed practical stability criterion, it is proven that the speed regulation error can be constrained to a bounded set containing zero in a finite time.
3) The speed estimation problem is further solved by designing a NSMO based on the NSMRL for PMSM systems. By simulation analysis, it is seen that our established method demonstrates better performance in suppressing speed fluctuations and improving estimation accuracy in comparison to the [23].

This article is organized as follows. In Section II, the NSMRL is designed and analyzed. Combined with the PMSM mathematical model, the NSMC is designed and a finite time stability proof is given in Section III. In Section IV, a NSMO is designed to estimate motor speed for PMSM systems. In Section V, the effectiveness of NSMRL and NSMO is verified by the simulation studies. Finally, the conclusion is summarized in Section VI.

Notation. $\mathbb{R}$ denotes the set of real numbers. $\mathbb{R}^n$ denotes the real N-dimensional space. $\|\cdot\|$ denotes the usual Euclidean norm of "$\cdot$". sgn denotes the signum function. sup$[X]$ denotes an upper bound of a set X.

II. NEW REACHING LAW DESIGN

SMC is a widely used control method due to its several advantages, such as insensitivity to disturbances, fast response speed, and low number of adjusting parameters. However, SMC suffers from a chattering problem caused by repeated traversals on the sliding mode surface. To inhibit chattering, the traditional exponential reaching law (TERL) is proposed, which can be expressed as [26]

$$\frac{ds}{dt} = -\epsilon\,\mathrm{sgn}(s) - \mathbf{k}s, \epsilon > 0, \mathbf{k} > 0, \tag{1}$$

where s shows a sliding mode surface function, $\epsilon\,\mathrm{sgn}(s)$ shows the isokinetic reaching law and $\mathbf{k}s$ shows the exponential reaching law.

However, since the parameters of TERL cannot be changed once they have been determined, the reduction of chattering and the convergence speed improvement cannot be achieved simultaneously. In [8], an improvement of TERL was defined as

$$\begin{cases} \dfrac{ds}{dt} = -\varepsilon\|x\|^{\alpha}\,\mathrm{sgn}(s) - \mathbf{k}\,|s|^{\mathfrak{h}\,\mathrm{sgn}(|s|-1)}\,s, \\ \lim\limits_{t\to\infty}\|x\| = 0, \varepsilon > 0, k > 0, 0 < \alpha < 1, 0 < \mathfrak{h} < 1. \end{cases} \tag{2}$$

To simplify the following description, (2) is referred to as Ref.

Although the designed controller based on (2) indeed can suppress chattering and accelerate the system convergence speed [8], finite time convergence is not guaranteed when the system is disturbed. To solve this problem, a new sliding mode reaching law is designed as follows

$$\begin{cases} \dfrac{ds}{dt} = -\epsilon Q(s)\,|s|^{\nu}\,\mathrm{sgn}(s) - \mathbf{k}\|x\|^{\mathfrak{h}\,\mathrm{sgn}(\|x\|-1)}s - \ell s, \\ Q(s) = |s| - (|s|-1)e^{-\chi|s|}, \end{cases} \tag{3}$$

where x represents the system states, $\epsilon > 0, \mathbf{k} > 0, \chi > 0, 0 < \nu < 1, 0 < \mathfrak{h} < 1, Q(s) > \frac{1}{e^x}$ and $\ell \geq 0$.

A brief analysis of (3) is made. From (3), when $|s| \geq 1$, there are two variable reaching laws $\epsilon Q(s)\,|s|^{\nu}$ with $Q(s) \geq 1$ and $\mathbf{k}\|x\|^{\mathfrak{h}}s + \ell s$. Thus a faster reaching speed is provided. In other words, the farther the system states are from the sliding mode surface, the faster the reaching speed will be ensured. On the contrary, when $|s| < 1$, the decay rate of $|s|$ is faster than $|s|^{\nu}$. Therefore, $\epsilon Q(s)\,|s|^{\nu}$ plays a main role. As $|s|$ tends to 0 and $Q(s)$ decreases to 1, the sliding mode gain is gradually reduced. It is effective for reducing chattering.

Remark 1: Unlike (1), a variable gain is introduced to (3). Therefore, a larger gain is provided to increase reaching speed when the system states are away from the sliding mode surface, but also a smaller gain is needed to reduce chattering when the system states are close to the sliding mode surface. Compared with (2), an additional variable gain is introduced in (3), which further improves convergence speed without increasing the chattering phenomenon. Additionally, an invariant gain is introduced to address the unknown disturbances.

A. THE NSMRL SIMULATION ANALYSIS

To better show the effectiveness of (3), we now use an example by comparing it with (1) and (2). Let us consider a typical second-order system, which is expressed as

$$\begin{cases} \dot{x}_1 = x_2, \\ \dot{x}_2 = -30x_2 + 140\mu(t) + 10\sin(\pi t). \end{cases} \tag{4}$$

For easy calculation, choose the sliding-mode surface function s as

$$s = cx_1 + x_2, \tag{5}$$

where $c > 0$. Substituting (4) into the derivative of (5), which can be shown as

$$\dot{s} = c\dot{x}_1 + \dot{x}_2 = cx_2 - 30x_2 + 140\mu(t) + 10\sin(\pi t). \tag{6}$$

Depending on the (3), the control law is obtained as

$$\begin{aligned}\mu(t) = -\frac{1}{140}[&cx_2 - 30x_2 + 10\sin(\pi t) \\ &+ \epsilon Q(s)\,|s|^{\nu}\,\mathrm{sgn}(s) + k\|x\|^{b\,\mathrm{sgn}(\|x\|-1)}s + \ell s].\end{aligned} \tag{7}$$

Choosing Lyapunov function $V = \frac{1}{2}s^2$, we get

$$\dot{V} = s[-\epsilon Q(s)\,|s|^{\nu}\,\mathrm{sgn}(s) - k\|x\|^{b\,\mathrm{sgn}(\|x\|-1)}s - \ell s]. \tag{8}$$

Defining $\frac{1}{e^x} = r$, (8) is rewritten as

$$\dot{V} + 2^{\frac{1+\nu}{2}}\epsilon r V^{\frac{1+\nu}{2}} \leq 0. \tag{9}$$

According to [29], the (4) convergence time T_s is

$$T_s \leq \frac{1}{2^{\frac{1+\nu}{2}}\epsilon r(1-\nu)}V(0)^{\frac{1-\nu}{2}}. \tag{10}$$

From (10), the system states converge to the sliding mode surface within a finite time has been rigorously proven.

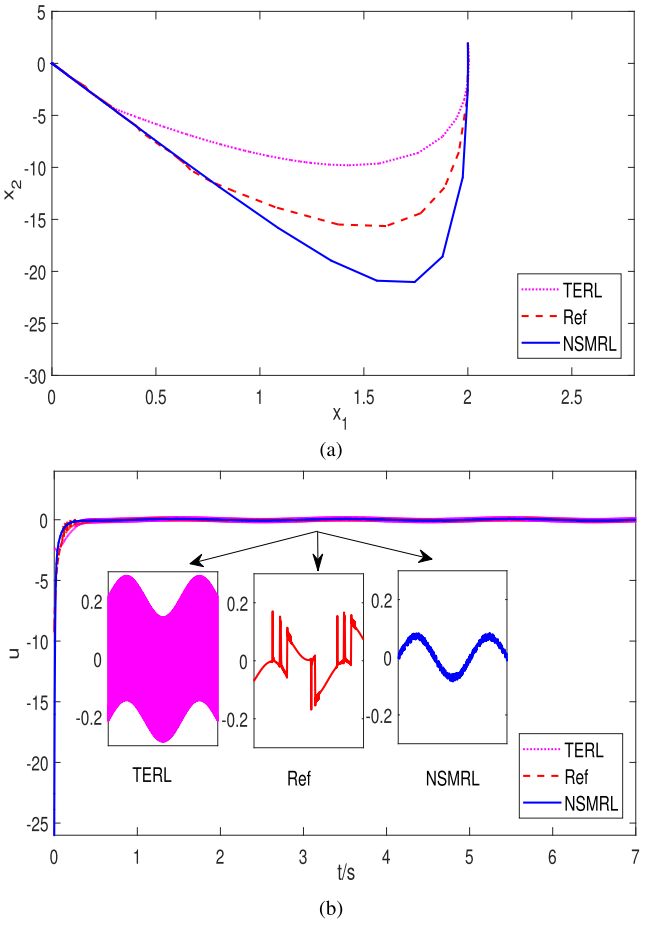

FIGURE 1. Performance comparison of TERL, Ref and NSMRL. (a)Phase trajectory. (b)Controller output.

To prove the effectiveness of NSMRL, the controllers designed according to (1) and (2) are

$$\begin{aligned}\mu_1(t) &= -\frac{1}{140}[cx_2 - 30x_2 + 10\sin(\pi t) + ks + \epsilon\,\mathrm{sgn}(s)], \\ \mu_2(t) &= -\frac{1}{140}[cx_2 - 30x_2 + 10\sin(\pi t) \\ &\quad + \epsilon\|x\|^{\alpha}\,\mathrm{sgn}(s) + k\,|s|^{b\,\mathrm{sgn}(|s|-1)}\,s].\end{aligned} \tag{11}$$

To draw the simulation results, the parameters are selected as follow: $c = 15, \epsilon = 30, b = 0.4, \ell = 0, \nu = 0.35, k = 10$ and $\chi = 500$. The initial state of this system $[x_1, x_2]$ is set to [2,2]. Fig. 1 shows the performance comparison between TERL, Ref and NSMRL. From Fig. 1 (a), we conclude that the system states converge to the sliding surface at the fastest speed through our proposed NSMRL. Fig. 1 (b) shows the controller output. Obviously, the chattering of the controller designed by our method is minimized.

III. THE SPEED CONTROLLER DESIGNED BASED ON NSMRL

A. MATHEMATICAL MODEL OF PMSM

Considering the complexity of the internal electrics of PMSMs, this paper makes some assumptions to simplify the

analysis. Ignoring the PMSM iron sore saturation and the eddy current and hysteresis, hence the mathematical model of the PMSM in the d-q rotating coordinate is expressed as [27]

$$\begin{cases} \dfrac{di_d}{dt} &= -\dfrac{R_s}{L_d}i_d + p_n w i_q + \dfrac{1}{L_d}u_d, \\ \dfrac{di_q}{dt} &= -\dfrac{R_s}{L_q}i_q - p_n w i_d + \dfrac{1}{L_q}u_q - \dfrac{p_n\psi_f}{L_q}w, \\ \dfrac{dw}{dt} &= \dfrac{3p_n\psi_f}{2J}i_q - \dfrac{B}{J}w - \dfrac{T_L}{J}, \end{cases} \tag{12}$$

where u_d, i_d and L_d are the stator voltage, stator current and inductance of d axes; u_q, i_q and L_q are the stator voltage and stator current, and inductance of q axes; R_s represents the stator resistance, p_n and w are the pole number of PMSMs and the mechanical angular velocity, respectively; T_L, ψ_f, J and B represent load torque, flux linkage, moment of inertia and viscosity coefficient, respectively.

B. DESIGN OF NSMC

In this subsection, the NSMC will be designed by a NSMRL to solve speed regulation for PMSMs.

Considering the parameter uncertainties and external disturbances, which are collectively referred to as lumped disturbances, from (12) the motor dynamic equation is rewritten as

$$\dot{w} = \Lambda i_q + d, \tag{13}$$

where $\Lambda = \frac{3p_n\psi_f}{2J}$ and d represents the lumped disturbances. Then, the motor speed tracking error is defined as

$$\begin{cases} x_1 &= w^* - w, \\ x_2 &= \dot{w}^* - \dot{w}, \end{cases} \tag{14}$$

where w^* is the given reference speed. Substituting (13) into (14), we get

$$\begin{aligned} x_2 = \dot{x}_1 &= \dot{w}^* - \dot{w} \\ &= \dot{w}^* - \Lambda i_q - d. \end{aligned} \tag{15}$$

In this paper, the nonsingular terminal sliding mode surface is chosen as follows [27]

$$s = x_1 + \frac{1}{J}\int_0^t x_1^{\frac{p}{q}} dt, \tag{16}$$

where $J > 0$, p and q are positive odd integers with $0 < p/q < 1$.

The derivative of (16) is computed as

$$\dot{s} = \dot{x}_1 + \frac{1}{J}x_1^{\frac{p}{q}} = \dot{w}^* - \Lambda i_q - d + \frac{1}{J}x_1^{\frac{p}{q}}. \tag{17}$$

Combining (3) and (17), i_q is easily deduced as

$$\begin{aligned} i_q = \frac{1}{\Lambda}[&\dot{w}^* - d + \frac{1}{J}x_1^{\frac{p}{q}} + \epsilon Q(s)\,|s|^{\nu}\,\mathrm{sgn}(s) \\ &+ \mathbf{k}\|x\|^{\mathfrak{h}\,\mathrm{sgn}(\|x\|-1)}s + \ell s]. \end{aligned} \tag{18}$$

Since d is unknown, the designed i_q in (18) is unavailable. Based on the PMSM system, an extended state observer (ESO) given as follows is applied to estimate d [28]

$$\begin{cases} \dot{z_1} &= z_2 - h_1(z_1 - w) + \Lambda i_q, \\ \dot{z_2} &= -h_2(z_1 - w). \end{cases} \tag{19}$$

In the above formula, the lumped disturbance is estimated by z_2. On this basis, we can complete the feed-forward compensation of the speed regulation of PMSM systems. The (18) is redesigned as

$$\begin{aligned} i_q = \frac{1}{\Lambda}[&\dot{w}^* - z_2 + \frac{1}{J}x_1^{\frac{p}{q}} + \epsilon Q(s)\,|s|^{\nu}\,\mathrm{sgn}(s) \\ &+ \mathbf{k}\|x\|^{\mathfrak{h}\,\mathrm{sgn}(\|x\|-1)}s + \ell s]. \end{aligned} \tag{20}$$

C. STABILITY ANALYSIS

Before giving the main result, some useful lemmas are proposed at first.

Lemma 1: [29]: Consider the system

$$\dot{y}(t) = f(y(t)), \tag{21}$$

where $f : \mathcal{D} \to \mathbb{R}^n$ is continuous on an open neighborhood $\mathcal{D}$ of the origin and $f(0) = 0$. Let $V : \mathcal{D} \to \mathbb{R}$, $k > 0$ and $a \in (0, 1)$. A neighborhood $\mathcal{U} \subset \mathcal{D}$ of the origin such that V is positive definite, and $\dot{V} + kV^a$ is negative semi-definite on $\mathcal{U}$. The system (21) is stable at origin and the stable time satisfies $T \leq \frac{1}{k(1-a)}V(0)^{1-a}$.

Lemma 2: [30]: Consider the following nonlinear system

$$\dot{x} = g(x, u). \tag{22}$$

Assume the existence of a continuous function $V(x)$ such that

$$\dot{V}(x) \leq -kV^a(x) + \eth, \tag{23}$$

where $k > 0$, $0 < a < 1$ and $0 < \eth < \infty$. The trajectory of system (24) is practical finite time stable. In other words, the trajectories of the closed-loop system converges to $\mathbf{O}$ in a finite time T such that

$$\begin{cases} T &\leq \dfrac{V^{1-a}(x(0))}{k\hbar(1-a)}, \\ \mathbf{O} &= \left\{x | V^a(x) \leq \dfrac{\eth}{(1-\hbar)k}\right\}, \end{cases} \tag{24}$$

where $0 < \hbar < 1$.

Lemma 3: Consider system (22). Assume that there is a continuous function $V(x)$ satisfying

$$\dot{V}^{\frac{q}{p}}(x) \leq -kV^{\frac{q+p}{2p}}(x) + \eth, \tag{25}$$

where $p < q$ are positive odd, $k > 0$ and $0 < \eth < \infty$. The system (22) converges to a bounded region within a finite time.

Proof: By choosing $\zeta \in (0, 1]$, the inequality (25) is expressed as

$$\dot{V}^{\frac{q}{p}}(x) \leq -\zeta kV^{\frac{q+p}{2p}}(x) - (1-\zeta)kV^{\frac{q+p}{2p}}(x) + \eth. \tag{26}$$

Case 1: When $x \in \mathbf{O}_2 = \left\{x|V^{\frac{q+p}{2p}}(x) > \frac{\eth}{(1-\zeta)k}\right\}$, there exists

$$(\dot{V})^{\frac{q}{p}} \leq -\zeta k V^{\frac{q+p}{2p}}, \tag{27}$$

which is equivalent to

$$\dot{V} \leq -(\zeta k)^{\frac{p}{q}} V^{\frac{p+q}{2q}}. \tag{28}$$

By Lemma 1, The trajectory of the system converges to $\mathbf{O}_1 = \left\{x|V^{\frac{q+p}{2p}}(x) \leq \frac{\eth}{(1-\zeta)k}\right\}$ within a finite time $T \leq \frac{V^{1-\frac{q+p}{2q}}(x(0))}{(\zeta k)^{\frac{p}{q}}(1-\frac{q+p}{2q})}$.

Case 2: When $x \in \mathbf{O}_1 = \left\{x|V^{\frac{q+p}{2p}}(x) \leq \frac{\eth}{(1-\zeta)k}\right\}$, by Case 1, $x(t)$ will always stay in $\mathbf{O}_1$.

In conclusion, the system state of (22) converges to $\mathbf{O}_1$ in a finite time T. ■

Theorem 1: When the parameters are met the following selection conditions, $\epsilon > 0$, $\mathbf{k} > 0$, $\ell \geq \frac{1}{2}$, $\chi > 0$, $0 < p/q < 1, 0 < \nu < 1$ and $0 < \mathfrak{h} < 1$, the speed regulation of PMSM systems is stable within a finite time.

Proof: First, we prove that the (16) converges to a bounded region in a finite time. Choose the Lyapunov function

$$V = \frac{1}{2}s^2. \tag{29}$$

By substituting the equation (17) into the time derivative of (29), it is shown as

$$\begin{aligned}\dot{V} &= s\dot{s} = s(\dot{x}_1 + \frac{1}{J}x_1^{\frac{p}{q}}) \\ &= s(\dot{w}^* - \Lambda i_q - d + \frac{1}{J}x_1^{\frac{p}{q}}).\end{aligned} \tag{30}$$

Substituting the equation (20) into (30) yields

$$\begin{aligned}\dot{V} = s\{&\dot{w}^* - [\dot{w}^* - z_2 + \frac{1}{J}x_1^{\frac{p}{q}} + \epsilon Q(s)\,|s|^{\nu}\,\mathrm{sgn}(s) \\ &+ \mathbf{k}\|x\|^{\mathfrak{h}\,\mathrm{sgn}(\|x\|-1)}s + \ell s] - d + \frac{1}{J}x_1^{\frac{p}{q}}\}.\end{aligned} \tag{31}$$

Assuming $|d - z_2| \leq \eta$, one obtains

$$\begin{aligned}\dot{V} &= -s[\epsilon Q(s)\,|s|^{\nu}\,\mathrm{sgn}(s) + \ell s + z_2 - d \\ &\quad + \mathbf{k}\|x\|^{\mathfrak{h}\,\mathrm{sgn}(\|x\|-1)}s] \\ &\leq -\epsilon e^{-\chi}\,|s|^{\nu+1}\,\mathrm{sgn}(s) - \mathbf{k}\|x\|^{\mathfrak{h}\,\mathrm{sgn}(\|x\|-1)}s^2 \\ &\quad - \ell s^2 + \eta\,|s| \\ &\leq -2^{\gamma}\epsilon e^{-\chi}V^{\gamma} - [\mathbf{k}\|x\|^{\mathfrak{h}\,\mathrm{sgn}(\|x\|-1)} + \ell - \frac{1}{2}]s^2 + \frac{\eta^2}{2},\end{aligned} \tag{32}$$

where $\gamma = \frac{1+\nu}{2}$. By choosing $\ell \geq \frac{1}{2}$, (32) is written as

$$\dot{V} \leq -2^{\gamma}\epsilon e^{-\chi}V^{\gamma} + \frac{\eta^2}{2}. \tag{33}$$

By Lemma 2, the (16) converges to D in a finite time T_s in which

$$\begin{cases} T_s & \leq \dfrac{V^{1-\gamma}(s(0))}{(1-\gamma)2^{\gamma}\epsilon e^{-\chi}\eth}, \\ D & = \left\{s|V(s) \leq \left[\dfrac{\eta^2}{(1-\eth)2^{1+\gamma}\epsilon e^{-\chi}}\right]^{\frac{1}{\gamma}}\right\}. \end{cases} \tag{34}$$

Then we prove the speed tracking error is bounded. Define $M = \int_0^t x_1^{\frac{p}{q}}dt$, $\bar{D} = \sup[D]$. Consider a Lyapunov function

$$V = \frac{1}{2}\left[\int_0^t x_1^{\frac{p}{q}}dt\right]^2 = \frac{1}{2}M^2. \tag{35}$$

Combining (16), we get

$$\dot{V} = (s - \frac{M}{J})^{\frac{p}{q}}M. \tag{36}$$

According to Young's inequality, the equation (36) is rewritten as

$$\begin{aligned}\dot{V}^{\frac{q}{p}} &\leq \left|\bar{D}\right|\,|M|^{\frac{q}{p}} - \frac{1}{J}\,|M|^{\frac{q+p}{p}} \\ &\leq G(\tau)\left|\bar{D}\right|^n + \tau[|M|^{\frac{q}{p}}]^m - \frac{1}{J}\,|M|^{\frac{q+p}{p}},\end{aligned} \tag{37}$$

where $\tau > 0$, $m = \frac{p+q}{q}$, $n = \frac{p+q}{p}$ and $G(\tau) = \frac{(m\tau)^{-\frac{n}{m}}}{n}$. Therefore, (37) becomes

$$\dot{V}^{\frac{q}{p}} \leq -2^{\frac{q+p}{2p}}(\frac{1}{J} - \tau)V^{\frac{q+p}{2p}} + G(\tau)\left|\bar{D}\right|^n. \tag{38}$$

Let $\frac{1}{J} > \tau$. By Lemma 3, we get the variable M converges to W in a finite time T in which

$$\begin{cases} T & \leq \dfrac{V^{1-\frac{q+p}{2q}}(M(0))}{[\zeta 2^{\frac{q+p}{2p}}(\frac{1}{J} - \tau)]^{\frac{p}{q}}(1-\frac{q+p}{2q})}, \\ W & = \left\{M|V(M) \leq \left[\dfrac{JG(\tau)\left|\bar{D}\right|^n}{(1-\tau J)(1-\zeta)2^{\frac{q+p}{2p}}}\right]^{\frac{2p}{q+p}}\right\}. \end{cases} \tag{39}$$

Define $\bar{W} = \sup[W]$. From (16), we have

$$x_1 = s - \frac{1}{J}\int_0^t x_1^{\frac{p}{q}}dt = s - \frac{M}{J}. \tag{40}$$

Based on (40) one has

$$x_1^2 \leq \bar{D}^2 + \frac{\bar{W}^2}{J^2} + 2\frac{\bar{D}\bar{W}}{J}.$$

Hence, the speed tracking error reaches a bounded region in a finite time $T_s + T$. When the individual parameters are determined, the speed tracking error and convergence time are determined. ■

Remark 2: In [8], the errors of disturbances observation and actual disturbances were ignored. Such a scenario is highly illogical in real-world applications. Hence, this paper addresses the scenario where non-zero errors between disturbances observations and actual values are considered.

IV. THE NSMO DESIGNED BASED ON NSMRL

In speed regulation of PMSM systems, accurately detecting the rotor position through mechanical sensors is crucial for its normal operation. However, traditional mechanical sensors are usually affected by external factors such as temperature and humidity, leading to inaccurate detections. Furthermore, it affects the overall performance of the systems. To solve this problem, the SMO is designed to replace the mechanical sensor. In industrial applications, the SMO is often used to estimate the stator current to obtain the back EMF [23]. To improve the dynamic performance of PMSM systems, a NSMO is presented to obtain the back EMF information more accurately. It is worth noting that the rotor position and speed information can be obtained using the arctangent function with the aid of the estimation of the back EMF.

A. DESIGN OF NSMO

Using the Clark transform, the mathematical model of PMSMs in the α-β coordinate axes is obtained as [22]

$$\begin{bmatrix} u_\alpha \\ u_\beta \end{bmatrix} = R_s \begin{bmatrix} i_\alpha \\ i_\beta \end{bmatrix} + L_s \frac{d}{dt} \begin{bmatrix} i_\alpha \\ i_\beta \end{bmatrix} + \begin{bmatrix} e_\alpha \\ e_\beta \end{bmatrix}, \tag{41}$$

where $[u_\alpha \quad u_\beta]^\top$, $[i_\alpha \quad i_\beta]^\top$ and $[e_\alpha \quad e_\beta]^\top$ represent the stator voltage, stator current and back EMF components on the axis α-β; R_s and L_s are the stator resistance and stator inductance, respectively. Back EMF force satisfies

$$\begin{bmatrix} e_\alpha \\ e_\beta \end{bmatrix} = w_e \psi_f \begin{bmatrix} -\sin\theta_e \\ \cos\theta_e \end{bmatrix}, \tag{42}$$

where w_e is electrical angular speed, θ_e is electrical angle.

To obtain the state equation for the stator current, from (41) there holds

$$\frac{d}{dt} \begin{bmatrix} i_\alpha \\ i_\beta \end{bmatrix} = -\frac{R_s}{L_s} \begin{bmatrix} i_\alpha \\ i_\beta \end{bmatrix} + \frac{1}{L_s} \begin{bmatrix} u_\alpha \\ u_\beta \end{bmatrix} - \frac{1}{L_s} \begin{bmatrix} e_\alpha \\ e_\beta \end{bmatrix}. \tag{43}$$

Define $\hat{i}_\alpha$ and $\hat{i}_\beta$ as the observation value of the stator current. Let $\tilde{i}_\alpha = \hat{i}_\alpha - i_\alpha$ and $\tilde{i}_\beta = \hat{i}_\beta - i_\beta$. According to (43) and (3), the NSMO is designed to observe the stator current as follows

$$\frac{d}{dt} \begin{bmatrix} \hat{i}_\alpha \\ \hat{i}_\beta \end{bmatrix} = -\frac{R_s}{L_s} \begin{bmatrix} \hat{i}_\alpha \\ \hat{i}_\beta \end{bmatrix} + \frac{1}{L_s} \begin{bmatrix} u_\alpha \\ u_\beta \end{bmatrix} - \frac{1}{L_s} \begin{bmatrix} v_\alpha \\ v_\beta \end{bmatrix}, \tag{44}$$

where v_α and v_β denote the sliding mode control law defined as

$$\begin{aligned} v_\alpha &= \epsilon_1 Q(\tilde{i}_\alpha) \left|\tilde{i}_\alpha\right|^\nu \operatorname{sgn}(\tilde{i}_\alpha) + \ell_1 \tilde{i}_\alpha, \\ v_\beta &= \epsilon_1 Q(\tilde{i}_\beta) \left|\tilde{i}_\beta\right|^\nu \operatorname{sgn}(\tilde{i}_\beta) + \ell_1 \tilde{i}_\beta. \end{aligned}$$

Then we have

$$\frac{d}{dt} \begin{bmatrix} \tilde{i}_\alpha \\ \tilde{i}_\beta \end{bmatrix} = -\frac{R_s}{L_s} \begin{bmatrix} \tilde{i}_\alpha \\ \tilde{i}_\beta \end{bmatrix} + \frac{1}{L_s} \begin{bmatrix} e_\alpha - v_\alpha \\ e_\beta - v_\beta \end{bmatrix}. \tag{45}$$

Through the NSMO designed above, the initial estimation of back EMF that named $\hat{e}_\alpha$ and $\hat{e}_\beta$ are obtained by v_α and v_β. In order to obtain more accurate rotor information, a back electromotive force observer (BEFO) is introduced to further process the initial estimation of back EMF information. The derivative of $\hat{e}_\alpha$, $\hat{e}_\beta$ and w_e with respect to (42) is obtained as

$$\begin{cases} \dfrac{d\hat{e}_\alpha}{dt} &= -w_e \hat{e}_\beta, \\ \dfrac{d\hat{e}_\beta}{dt} &= w_e \hat{e}_\alpha, \\ \dfrac{dw_e}{dt} &= 0. \end{cases} \tag{46}$$

The sampling frequency in the actual system is far greater than the rate of speed change rate. Therefore, it is assumed that the speed of PMSMs is a constant value within a sampling cycle. Define $\hat{E}_\alpha$, $\hat{E}_\beta$ and $\hat{w}_e$ as the result of further processing of $\hat{e}_\alpha$, $\hat{e}_\beta$ and electrical angular speed. Let $\tilde{E}_\alpha = \hat{E}_\alpha - \hat{e}_\alpha$, $\tilde{E}_\beta = \hat{E}_\beta - \hat{e}_\beta$ and $\tilde{w}_e = \hat{w}_e - w_e$. A BEFO is constructed based on (3) and (46) as follows

$$\begin{cases} \dfrac{d\hat{E}_\alpha}{dt} &= -\hat{w}_e \hat{E}_\beta - \epsilon_2 Q(\tilde{E}_\alpha) \left|\tilde{E}_\alpha\right|^{\nu_1} \operatorname{sgn}(\tilde{E}_\alpha), \\ \dfrac{d\hat{E}_\beta}{dt} &= \hat{w}_e \hat{E}_\alpha - \epsilon_2 Q(\tilde{E}_\beta) \left|\tilde{E}_\beta\right|^{\nu_1} \operatorname{sgn}(\tilde{E}_\beta), \\ \dfrac{d\hat{w}_e}{dt} &= \hat{E}_\beta \tilde{E}_\alpha - \hat{E}_\alpha \tilde{E}_\beta. \end{cases} \tag{47}$$

According to (46) and (47), it is deduced that

$$\begin{cases} \dfrac{d\tilde{E}_\alpha}{dt} &= -\hat{w}_e \hat{E}_\beta - \epsilon_2 Q(\tilde{E}_\alpha) \left|\tilde{E}_\alpha\right|^{\nu_1} \operatorname{sgn}(\tilde{E}_\alpha) + w_e \hat{e}_\beta, \\ \dfrac{d\tilde{E}_\beta}{dt} &= \hat{w}_e \hat{E}_\alpha - \epsilon_2 Q(\tilde{E}_\beta) \left|\tilde{E}_\beta\right|^{\nu_1} \operatorname{sgn}(\tilde{E}_\beta) - w_e \hat{e}_\alpha, \\ \dfrac{dw_e}{dt} &= \hat{E}_\beta \tilde{E}_\alpha - \hat{E}_\alpha \tilde{E}_\beta, \end{cases} \tag{48}$$

where $\epsilon_2 > 0$ and $0 < \nu_1 < 1$.

Since the back EMF estimation information (47) is usually contaminated by various noises, we then use a low-pass filter [31] to eliminate them. The estimation value of the speed of PMSMs is calculated by

$$\hat{w}_e = \frac{\sqrt{\hat{E}_\alpha^2 + \hat{E}_\beta^2}}{\psi_f}. \tag{49}$$

The estimation information of rotor position is preliminarily obtained

$$\hat{\theta}_{eqe} = \arctan\left(\frac{-\hat{E}_\alpha}{\hat{E}_\beta}\right). \tag{50}$$

Since a low-pass filter is introduced, phase compensation is required. Therefore, the final formula for calculating the rotor position information of the motor is expressed as

$$\hat{\theta}_e = \hat{\theta}_{eqe} + \arctan\left(\frac{\hat{w}_e}{w_c}\right), \tag{51}$$

where w_c is the cut-off frequency of the low-pass filter.

B. STABILITY ANALYSIS

Theorem 2: When the parameters are chosen as $\epsilon_1 > 0$, $\epsilon_2 > 0$, $\ell_1 \geq \frac{1}{2}$, $\chi > 0$, $0 < \nu < 1$ and $0 < \nu_1 < 1$, the observation error of the NSMO and the BEFO are convergent.

Proof: Letting $V_1(\tilde{i}_\alpha) = \frac{1}{2}\tilde{i}_\alpha^2$ and $V_2(\tilde{i}_\beta) = \frac{1}{2}\tilde{i}_\beta^2$, the Lyapunov function is constructed as

$$V(\tilde{i}_\alpha, \tilde{i}_\beta) = \frac{1}{2}\tilde{i}_\alpha^2 + \frac{1}{2}\tilde{i}_\beta^2 = V_1(\tilde{i}_\alpha) + V_2(\tilde{i}_\beta). \tag{52}$$

Substituting the equation (45) into the time derivative of (52), one has

$$\begin{aligned}\dot{V}(\tilde{i}_\alpha, \tilde{i}_\beta) = \tilde{i}_\alpha[\frac{1}{L_s}(-R_s\tilde{i}_\alpha + e_\alpha - v_\alpha)] \\ + \tilde{i}_\beta[\frac{1}{L_s}(-R_s\tilde{i}_\beta + e_\beta - v_\beta)].\end{aligned} \tag{53}$$

Substituting the v_α and v_β into (53), we can get

$$\begin{aligned}\dot{V} &= \tilde{i}_\alpha[\frac{1}{L_s}(-R_s\tilde{i}_\alpha + e_\alpha - v_\alpha)] \\ &\quad + \tilde{i}_\beta[\frac{1}{L_s}(-R_s\tilde{i}_\beta + e_\beta - v_\beta)] \\ &= \frac{\tilde{i}_\alpha}{L_s}[e_\alpha - \epsilon_1 Q(\tilde{i}_\alpha)\left|\tilde{i}_\alpha\right|^\nu \operatorname{sgn}(\tilde{i}_\alpha) - \ell_1\tilde{i}_\alpha] \\ &\quad + \frac{\tilde{i}_\beta}{L_s}[e_\beta - \epsilon_1 Q(\tilde{i}_\beta)\left|\tilde{i}_\beta\right|^\nu \operatorname{sgn}(\tilde{i}_\beta) - \ell_1\tilde{i}_\beta] \\ &\quad - \frac{R_s}{L_s}(\tilde{i}_\alpha^2 + \tilde{i}_\beta^2) \\ &= \dot{V}_1 + \dot{V}_2.\end{aligned} \tag{54}$$

Assuming $\gamma = \frac{1+\nu}{2}$, it holds

$$\begin{aligned}\dot{V}_1 &\leq \frac{1}{L_s}[-\epsilon_1 e^{-\chi}\left|\tilde{i}_\alpha\right|^{\nu+1} - \ell_1\tilde{i}_\alpha^2 + \left|\tilde{i}_\alpha\right||e_\alpha|] \\ &\leq -\frac{1}{L_s}[2^\gamma\epsilon_1 e^{-\chi}V_1^\gamma - \frac{1}{2}e_\alpha^2 + (\ell_1 - \frac{1}{2})\tilde{i}_\alpha^2].\end{aligned} \tag{55}$$

By Theorem 1, the observation error of stator current on the axis α converges to D_1 in a finite time T_{s_α} in witch

$$\begin{cases} T_{s_\alpha} & \leq \dfrac{L_s V_1^{1-\gamma}(\tilde{i}_\alpha(0))}{(1-\gamma)2^\gamma\epsilon_1 e^{-\chi}\eth_1}, \\ D_1 & = \left\{\tilde{i}_\alpha | V(\tilde{i}_\alpha) \leq \left[\dfrac{e_\alpha^2}{(1-\eth_1)2^{1+\gamma}\epsilon_1 e^{-\chi}}\right]^{\frac{1}{\gamma}}\right\}. \end{cases} \tag{56}$$

Similarly, similar results can be obtained by analyzing V_2.

To prove that the observation error of the BEFO is convergent, the Lyapunov function is defined

$$V = \frac{1}{2}\tilde{E}_\alpha^2 + \frac{1}{2}\tilde{E}_\beta^2 + \frac{1}{2}\tilde{w}_e^2. \tag{57}$$

Substituting the equation (48) into the time derivative of (57), we have

$$\dot{V} = -\epsilon_2 Q(\tilde{E}_\alpha)\left|\tilde{E}_\alpha\right|^{\nu_1+1} - \epsilon_2 Q(\tilde{E}_\beta)\left|\tilde{E}_\beta\right|^{\nu_1+1}. \tag{58}$$

TABLE 1. Parameters of the motor.

Parameter and Unit	Value
DC power $V_d c\ V$	311
Inductance $L_d = L_q / mH$	8.5
Stator phase resistance R/Ω	2.875
Viscous friction coefficient $B/N \cdot m \cdot s$	0.002
Rotational inertia $J/kg \cdot m^2$	0.001
Flux linkage of permanent magnets ψ_f / Wb	0.175

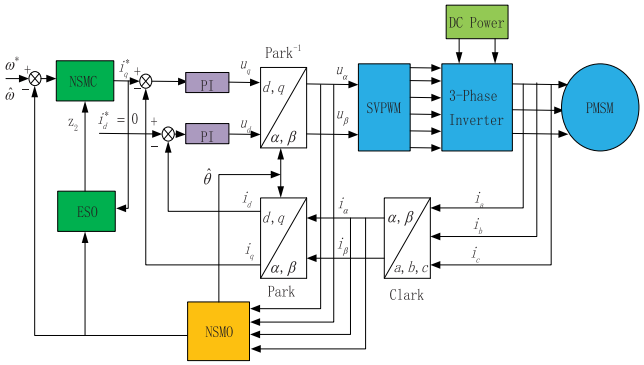

FIGURE 2. The block diagram of PMSM speed regulation system.

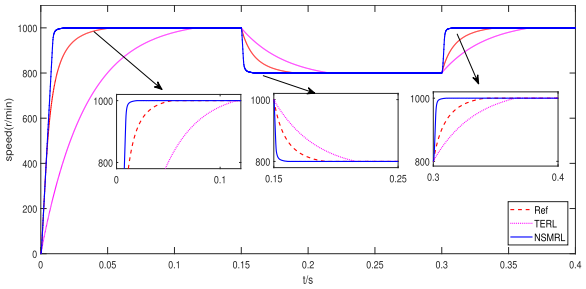

FIGURE 3. Simulation waveforms of speed change.

When $\epsilon_2 > 0$, there is $\dot{V} \leq 0$. Based on Lyapunov stability theory, the BEFO observation error system is stable. ■

V. SIMULATION AND RESULT

In this section, to draw the simulation results, we use vector control $i_d = 0$. The Table 1 shows motor parameters in this paper and the Fig. 2 is a block diagram of the speed regulation of the PMSM system. In order to illustrate the effectiveness of our proposed method in this paper, the developed NSMC is compared with the traditional sliding mode controller (TSMC) and the reference sliding mode controller (RSMC) designed by TERL and Ref, respectively. The TSMC and RSMC are written as

$$\begin{aligned} i_{q1} &= \frac{1}{\Lambda}[\dot{w}^* - z_2 + \frac{1}{J}x_1^{\frac{p}{q}} + \epsilon\operatorname{sgn}(s) + \mathbf{k}s], \\ i_{q2} &= \frac{1}{\Lambda}[\dot{w}^* - z_2 + \frac{1}{J}x_1^{\frac{p}{q}} + \epsilon\|x\|^\alpha\operatorname{sgn}(s) \\ &\quad + \mathbf{k}\left|s\right|^{\mathfrak{h}\operatorname{sgn}(|s|-1)}s]. \end{aligned}$$

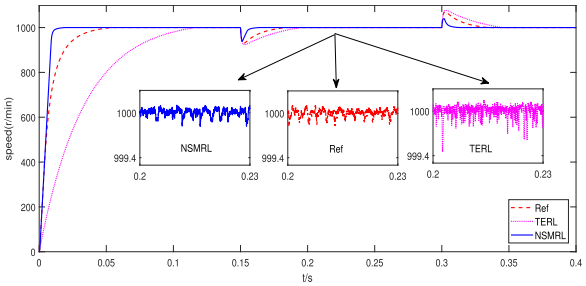

FIGURE 4. Load change speed simulation diagram.

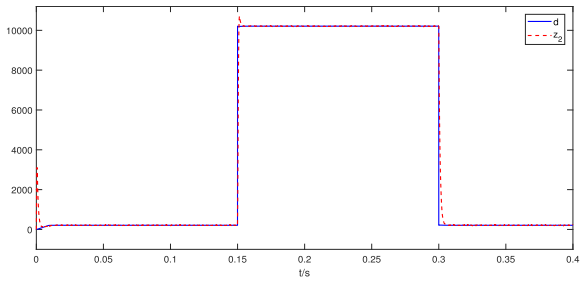

FIGURE 5. Simulation results of ESO.

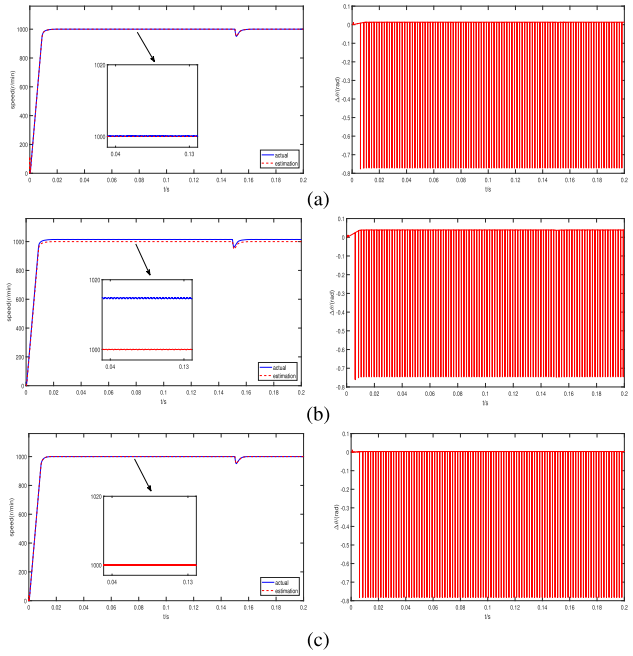

FIGURE 6. Simulation waveforms of motor speed and rotor position angle error. (a) NSMO. (b) TSMO. (c)NSMO+BEFO.

The NSMO is compared with traditional sliding mode observer (TSMO) designed in [23], which is expressed as

$$\frac{d}{dt}\begin{bmatrix}\hat{i}_\alpha\\ \hat{i}_\beta\end{bmatrix} = -\frac{R_s}{L_s}\begin{bmatrix}\hat{i}_\alpha\\ \hat{i}_\beta\end{bmatrix} + \frac{1}{L_a}\begin{bmatrix}u_\alpha\\ u_\beta\end{bmatrix} - \frac{1}{L_s}\begin{bmatrix}H(\tilde{i}_\alpha)\\ H(\tilde{i}_\beta)\end{bmatrix},$$

where

$$H(\tilde{i}_\alpha) = \frac{2}{1+e^{-\tilde{i}_\alpha}} - 1, H(\tilde{i}_\beta) = \frac{2}{1+e^{-\tilde{i}_\beta}} - 1.$$

Some parameters are chosen as follow: $p = 3$, $q = 5$, $\nu = 0.3$, $\nu_1 = 0.001$, $\mathfrak{h} = 0.4$, $\epsilon = 100$, $\epsilon_1 = 420$, $\epsilon_2 = 40000$, $\jmath = 10000$, $\chi = 1$, $\mathbf{k} = 30$, and $\ell_1 = 10000$. The simulation time T and reference speed are 0.4s and 1000 r/min, respectively.

Fig. 3 shows the PMSM speed waveform. When adopting NSMRL, Ref and TERL, the time for motor speed to reach a given value is 0.019s, 0.05s and 0.115s, respectively. At 0.15s the reference speed decreases to 800 r/min suddenly, the adjustment time under NSMRL, Ref and TERL are about 0.01s, 0.04s and 0.065s. Obviously, ours is the best among these methods. When the load torque changes, the motor speed is shown in Fig. 4. The speed drop under NSMRL, Ref and TERL is 62r/min, 75r/min and 81r/min, respectively. This implies that our proposed method exhibits stronger robustness. From Fig. 5, it is seen that z_2 accurately and quickly track the disturbances. It is obviously shown in Fig. 6 that the speed estimation error of TSMO is bigger than that of NSMO and NSMO+BEFO. And the estimation error for rotor angle based on NSMO, TSMO and NSMO+BEFO are about 0.014rad, 0.04rad and 0.003rad, respectively. Obviously, our method is more effective.

VI. CONCLUSION

In this paper, a NSMRL has been proposed to improve the system convergence speed without serious chattering. Under the NSMRL, a NSMC has been designed to decrease the adjustment time and motor speed chattering for the speed regulation of PMSM system. In addition, a NSMO based on NSMRL has been constructed to obtain more accurate information of back EMF. Simulation results have verified the feasibility of this paper proposed methods.

REFERENCES

[1] C.-S. Park, J.-H. Kim, S.-H. Park, and M.-S. Lim, "Effect of electromagnetic force caused by PMSM on the vibration/noise of reciprocating compressors," *IEEE Access*, vol. 11, pp. 56324–56335, 2023.

[2] K.-H. Kim and M.-J. Youn, "A nonlinear speed control for a PM synchronous motor using a simple disturbance estimation technique," *IEEE Trans. Ind. Electron.*, vol. 49, no. 3, pp. 524–535, Jun. 2002.

[3] T. Jiao, W. X. Zheng, and S. Xu, "On stability of a class of switched nonlinear systems subject to random disturbances," *IEEE Trans. Circuits Syst. I, Reg. Papers*, vol. 63, no. 12, pp. 2278–2289, Dec. 2016.

[4] J.-K. Seok, J.-K. Lee, and D.-C. Lee, "Sensorless speed control of nonsalient permanent-magnet synchronous motor using rotor-position-tracking PI controller," *IEEE Trans. Ind. Electron.*, vol. 53, no. 2, pp. 399–405, Apr. 2006.

[5] H. Ding, X. Zou, and J. Li, "Sensorless control strategy of permanent magnet synchronous motor based on fuzzy sliding mode observer," *IEEE Access*, vol. 10, pp. 36743–36752, 2022.

[6] X. Ba, P. Wang, C. Zhang, J. G. Zhu, and Y. Guo, "Improved deadbeat predictive current control to enhance the performance of the drive system of permanent magnet synchronous motors," *IEEE Trans. Appl. Supercond.*, vol. 31, no. 8, pp. 1–4, Nov. 2021.

[7] S. Lu and X. Wang, "Observer-based command filtered adaptive neural network tracking control for fractional-order chaotic PMSM," *IEEE Access*, vol. 7, pp. 88777–88788, 2019.

[8] Y. Wang, Y. Feng, X. Zhang, and J. Liang, "A new reaching law for antidisturbance sliding-mode control of PMSM speed regulation system," *IEEE Trans. Power Electron.*, vol. 35, no. 4, pp. 4117–4126, Apr. 2020.

[9] T. H. Nguyen, T. T. Nguyen, V. Q. Nguyen, K. M. Le, H. N. Tran, and J. W. Jeon, "An adaptive sliding-mode controller with a modified reduced-order proportional integral observer for speed regulation of a permanent magnet synchronous motor," *IEEE Trans. Ind. Electron.*, vol. 69, no. 7, pp. 7181–7191, Jul. 2022.
[10] T. Jiao, W. X. Zheng, and S. Xu, "Unified stability criteria of random nonlinear time-varying impulsive switched systems," *IEEE Trans. Circuits Syst. I, Reg. Papers*, vol. 67, no. 9, pp. 3099–3112, Sep. 2020.
[11] X. Guo, S. Huang, and Y. Peng, "Robust speed sliding mode control for PMSM based on a novel reaching law and high-order fast terminal sliding-mode observer," in *Proc. 12th IEEE PES Asia–Pacific Power Energy Eng. Conf. (APPEEC)*, Sep. 2020, pp. 1–5.
[12] F. M. Zaihidee, S. Mekhilef, and M. Mubin, "Application of fractional order sliding mode control for speed control of permanent magnet synchronous motor," *IEEE Access*, vol. 7, pp. 101765–101774, 2019.
[13] C. Xu, K. Wang, X. Yang, and B. Zhang, "Terminal sliding mode control of permanent magnet synchronous motor based on a novel adaptive reaching law," in *Proc. IEEE 4th Adv. Inf. Manage., Communicates, Electron. Autom. Control Conf. (IMCEC)*, vol. 4, Jun. 2021, pp. 1731–1735.
[14] X. Xing and H. Sheng, "PMSM sliding mode control based on a new exponential reaching law," in *Proc. 3rd Int. Academic Exchange Conf. Sci. Technol. Innov. (IAECST)*, Dec. 2021, pp. 199–203.
[15] K. B. Devika and S. Thomas, "Power rate exponential reaching law for enhanced performance of sliding mode control," *Int. J. Control, Autom. Syst.*, vol. 15, no. 6, pp. 2636–2645, Dec. 2017.
[16] A. K. Junejo, W. Xu, C. Mu, M. M. Ismail, and Y. Liu, "Adaptive speed control of PMSM drive system based a new sliding-mode reaching law," *IEEE Trans. Power Electron.*, vol. 35, no. 11, pp. 12110–12121, Nov. 2020.
[17] M. S. Rafaq, F. Mwasilu, J. Kim, H. H. Choi, and J.-W. Jung, "Online parameter identification for model-based sensorless control of interior permanent magnet synchronous machine," *IEEE Trans. Power Electron.*, vol. 32, no. 6, pp. 4631–4643, Jun. 2017.
[18] F. Auger, M. Hilairet, J. M. Guerrero, E. Monmasson, T. Orlowska-Kowalska, and S. Katsura, "Industrial applications of the Kalman filter: A review," *IEEE Trans. Ind. Electron.*, vol. 60, no. 12, pp. 5458–5471, Dec. 2013.
[19] Y. Zhao, Z. Zhang, W. Qiao, and L. Wu, "An extended flux model-based rotor position estimator for sensorless control of salient-pole permanent-magnet synchronous machines," *IEEE Trans. Power Electron.*, vol. 30, no. 8, pp. 4412–4422, Aug. 2015.
[20] D. Yang, G. Zong, Y. Shi, and P. Shi, "Model reference adaptive tracking control of uncertain Markovian hybrid switching systems," *SIAM J. Control Optim.*, vol. 61, no. 2, pp. 434–457, 2023.
[21] Y. Zuo, C. Lai, and K. L. V. Iyer, "A review of sliding mode observer based sensorless control methods for PMSM drive," *IEEE Trans. Power Electron.*, vol. 38, no. 9, pp. 11352–11367, May 2023.
[22] G. Liu, H. Zhang, and X. Song, "Position-estimation deviation-suppression technology of PMSM combining phase self-compensation SMO and feed-forward PLL," *IEEE J. Emerg. Sel. Topics Power Electron.*, vol. 9, no. 1, pp. 335–344, Feb. 2021.
[23] N. Ren, L. Fan, and Z. Zhang, "Sensorless PMSM control with sliding mode observer based on sigmoid function," *J. Electr. Eng. Technol.*, vol. 16, no. 2, pp. 933–939, Mar. 2021.
[24] D. Liang, J. Li, and R. Qu, "Sensorless control of permanent magnet synchronous machine based on second-order sliding-mode observer with online resistance estimation," *IEEE Trans. Ind. Appl.*, vol. 53, no. 4, pp. 3672–3682, Jul. 2017.
[25] Y. Wang, J. Wu, Z. Guo, C. Xie, J. Liu, and X. Jin, "Flux-weakening fuzzy adaptive ST-SMO sensorless control algorithm for PMSM in EV," *J. Supercomput.*, vol. 78, no. 8, pp. 10930–10949, May 2022.
[26] W. Gao and J. C. Hung, "Variable structure control of nonlinear systems: A new approach," *IEEE Trans. Ind. Electron.*, vol. 40, no. 1, pp. 45–55, 1993.
[27] S. Li, M. Zhou, and X. Yu, "Design and implementation of terminal sliding mode control method for PMSM speed regulation system," *IEEE Trans. Ind. Informat.*, vol. 9, no. 4, pp. 1879–1891, Nov. 2013.
[28] T. A. Khaled, O. Akhrif, and I. A. Bonev, "Dynamic path correction of an industrial robot using a distance sensor and an ADRC controller," *IEEE/ASME Trans. Mechatronics*, vol. 26, no. 3, pp. 1646–1656, Jun. 2021.
[29] S. P. Bhat and D. S. Bernstein, "Continuous finite-time stabilization of the translational and rotational double integrators," *IEEE Trans. Autom. Control*, vol. 43, no. 5, pp. 678–682, May 1998.
[30] Z. Zheng, Y. Xia, and M. Fu, "Attitude stabilization of rigid spacecraft with finite-time convergence," *Int. J. Robust Nonlinear Control*, vol. 21, no. 6, pp. 686–702, 2011.
[31] K.-L. Kang, J.-M. Kim, K.-B. Hwang, and K.-H. Kim, "Sensorless control of PMSM in high speed range with iterative sliding mode observer," in *Proc. 19th Annu. IEEE Appl. Power Electron. Conf. Exposit. (APEC)*, 2004, pp. 1111–1116.

HANQING WANG received the B.Eng. degree from the School of Electrical and Electronic Engineering, Shandong University of Technology, China, in 2021, where he is currently pursuing the M.Eng. degree. His current research interests include power electronics and electric machine drives.

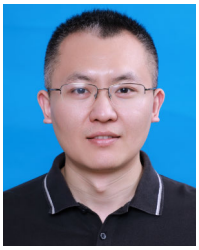

TICAO JIAO received the B.Sc. and M.Sc. degrees from the School of Mathematics and Institute of Automation, Qufu Normal University, Qufu, China, in 2008 and 2012, respectively, and the Ph.D. degree in control theory and control engineering from the Nanjing University of Science and Technology, Nanjing, China, in June 2016. He is currently a Professor with the School of Electrical and Electronic Engineering, Shandong University of Technology, China. His current research interests include stochastic systems and switched systems.

XUENING XING received the master's degree in control theory and control engineering from the Zhejiang University of Technology, Hangzhou, China, in 2005. He is currently an Associate Professor with the Shandong University of Technology, Zibo, China. His main research interests include computer control technology, intelligence of systems, and algorithms.

YANGUANG YANG received the B.Eng. degree in electrical engineering and automation from Fuzhou University, in 2009, and the M.Eng. degree in electrical engineering from Qingdao University, in 2015. He is currently a Senior Engineer with Changyi Power Supply Company, Shandong, China.